



Sea-level changes and paleoenvironmental responses in a coastal Florida salt marsh over the last three centuries

Carina Seitz · William F. Kenney · Brittany Patterson-Boyarski · Jason H. Curtis · María I. Vélez · Katie Glodzik · Jaime Escobar · Mark Brenner

Received: 19 April 2022 / Accepted: 28 November 2022 / Published online: 21 January 2023
© The Author(s), under exclusive licence to Springer Nature B.V. 2023

Abstract Florida’s coastal salt marshes are vulnerable to both direct and indirect human impacts, including climate change and consequent sea-level rise. For a salt marsh to survive in the face of ongoing sea-level rise, organic and/or mineral sediment must accumulate at a rate equal to or faster than that of sea-level increase. We explored the effects of Late Holocene sea-level variations in the Suwannee River Estuary within the Big Bend region of Florida (USA).

We conducted a paleoenvironmental study of a sediment core collected from a salt marsh near Cedar Key, on Florida’s Gulf of Mexico coast. The core spans the last ~320 years of sediment accumulation. Carbon isotope ($\delta^{13}\text{C}$) data and diatom assemblages indicate the salt marsh was relatively stable during that time frame and was dominated by C3 vegetation, likely *Juncus roemerianus*, but experienced moderate variations in salinity that likely reflect changes in sea-level, with an increase in salinity and marine incursions between ~1850 and 1930 CE. Whereas small vertical changes in sea-level have the potential to inundate large areas of the low-gradient salt marsh,

Supplementary Information The online version contains supplementary material available at <https://doi.org/10.1007/s10933-022-00275-4>.

C. Seitz (✉)
IPATEC, (CONICET-UNCO), Avenida De Los Pioneros
2350, 8400 San Carlos de Bariloche, Argentina
e-mail: cseitz@comahue-conicet.gob.ar

C. Seitz
Centro Regional Universitario Bariloche (CRUB),
Universidad Nacional del Comahue, Quintral 1250,
8400 San Carlos de Bariloche, Argentina

C. Seitz
Department of Geology, Universidad Nacional del Sur,
Avenida Alem 1253, B8000CPB Bahía Blanca, Argentina

W. F. Kenney · J. H. Curtis · M. Brenner
Land Use and Environmental Change Institute, University
of Florida, Gainesville, FL 32611, USA

B. Patterson-Boyarski · M. I. Vélez
Department of Geology, University of Regina,
Saskatchewan S4S 0A2, Canada

J. H. Curtis · M. Brenner
Department of Geological Sciences, University of Florida,
Gainesville, FL 32611, USA

K. Glodzik
School of Forest, Fisheries & Geomatics Sciences,
University of Florida, Gainesville, FL 32603, USA

J. Escobar
Department of Civil and Environmental Engineering,
Universidad del Norte, Barranquilla, Colombia

J. Escobar
Center for Tropical Paleocology and Archaeology,
Smithsonian Tropical Research Institute, Box 0843-03092,
Balboa, Panama

as observed during the interval ~1850–1930 CE, the salt-marsh vegetation recovered quickly after 1930 CE, indicating that the rate of aggradation and vegetation growth kept pace with the rate of sea-level rise. Despite the apparent resiliency of Big Bend salt marshes and likelihood that they will persist through accretion and migration, we expect to see major changes in salt-marsh ecology if rates of sea-level rise continue to accelerate.

Keywords Diatoms · Sediment lithology · Stable isotopes · Sea-level rise · Aggradation · Salinity

Introduction

Subtropical salt marshes occur along low-energy shorelines on Florida's Gulf of Mexico coast, at the mouths of rivers, and in bays, bayous and sounds (Florida Department of Environmental Protection 2020). These salt marshes are intertidal habitats that provide food, refuge, and nursery areas for numerous economically important taxa, including shrimp, blue crabs, and many finfish species (Zedler and Kercher 2005; Barbier et al. 2011). Salt marshes also provide other ecosystem services, in that they prevent shoreline erosion by buffering wave action and trapping sediment (Möller et al. 1999; Mudd et al. 2010). Salt-marsh ecosystems were considered to be highly vulnerable to sea-level rise, with static models predicting the imminent loss of 20–60% of coastal wetlands worldwide (Nicholls et al. 2007; Craft et al. 2009). Nevertheless, subsequent studies showed that salt marshes are in fact dynamic and less vulnerable than originally believed (Kirwan et al. 2016). Their long-term stability results from interactions among sea-level, land elevation, primary production, and sediment accretion (Morris et al. 2002). Those interactions are complex and lack linear feedback mechanisms (Kirwan et al. 2010). For instance, contrary to expectations, Morris et al. (2002) found that vegetation at low elevations grew faster during anomalously high sea-level years, possibly because of greater organic and mineral accretion and limited erosion.

Florida's west coast salt marshes are vulnerable to both direct and indirect human impacts. In some areas, residential development has destroyed upstream, freshwater tidal zones (Adam 2016). Salt marshes are also affected by climate change and

consequent sea-level response. For a salt marsh to survive in the face of ongoing sea-level rise, sediment (organic and mineral) must accumulate at a rate equal to or faster than that of sea-level increase. If sediment accretion cannot keep pace with the rate of water rise, marsh plants may be drowned and the area will be transformed into an open-water, muddy habitat (Sanger and Parker 2016). Additionally, salt marshes in some areas may transition into mangrove forests as the climate warms and mangroves migrate poleward (Saintilan et al. 2014; Giri and Long 2016; Cavanaugh et al. 2019).

Tide-gauge records from around Florida show that sea-level has risen at a mean rate of ~2.1–2.4 mm a⁻¹ during the last century, with accelerations in rate between 1928 and 1948, and again since 2000 (Mitchum et al. 2017). Some studies have looked at the impact of accelerating sea-level rise on Florida's coastal forests (Williams et al. 1999; DeSantis et al. 2007; Langston et al. 2017), but only a few investigations have compared the rate of sea-level rise to the rate of sediment accretion (Smoak et al. 2013; Breithaupt 2014; Vaughn et al. 2020, 2021) or explored how sea-level rise has affected the plant community in coastal salt marshes (Morris et al. 2002; Meirland et al. 2015).

The Big Bend's extremely flat topography, along with its low sediment supply, predisposes it to be highly susceptible to changes from sea-level rise (Hine et al. 1988; Kirwan and Megonigal 2013). Despite its overall relatively pristine condition, this ecologically unique region has experienced large-scale changes, including salt-marsh erosion, coastal forest die-off and replacement by inland-migrating salt marsh, and substantial oyster-reef collapse (Williams et al. 1999; Geselbracht et al. 2011; Seavey et al. 2011; Raabe and Stumpf 2016). Studies indicate that these changes are induced by sea-level rise and reduced freshwater discharge into the estuaries, though the interplay between these drivers is unclear (Seavey et al. 2011; Raabe and Stumpf 2016). These uncertainties and the ecological significance of this coastline served as primary motivations to examine Big Bend salt marsh responses to sea-level rise and salinity change. Our goal in this “paleo” study was to conduct a preliminary investigation of the effects of sea-level variations during the last few centuries on the physical and biological characteristics of the Suwannee Estuary salt marsh near Cedar Key,

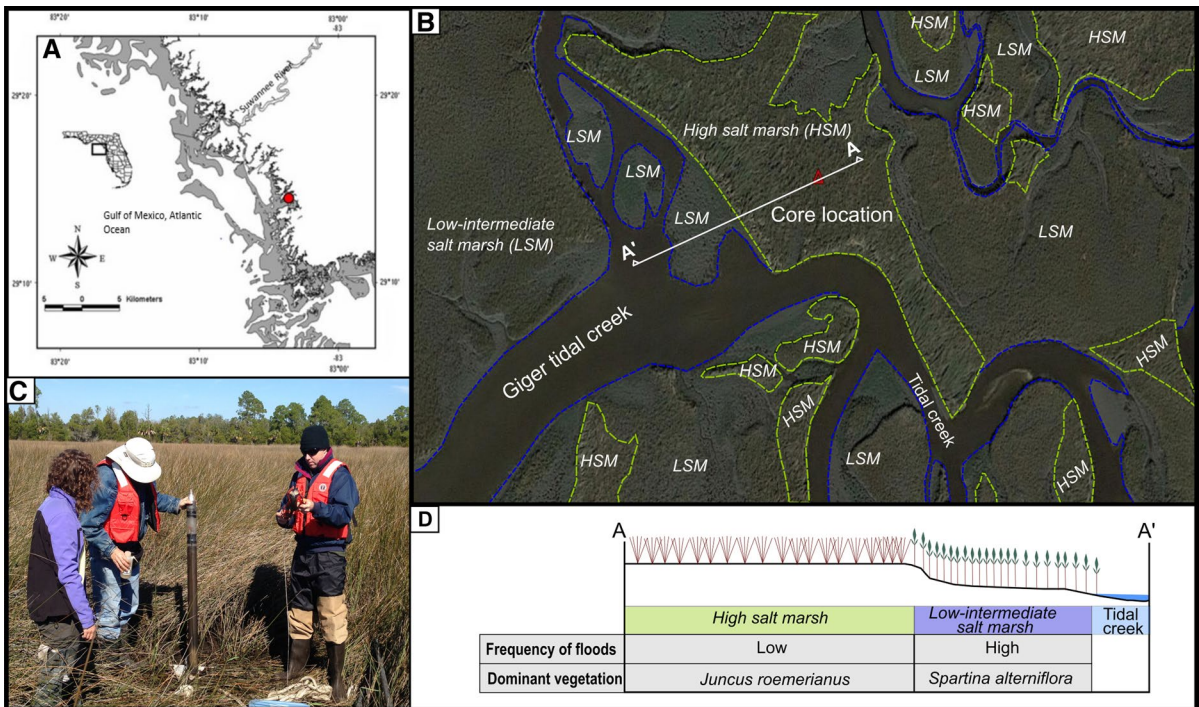


Fig. 1 **A** Map of the Suwannee River Estuary off the west coast of Florida, USA. Red dot indicates the location of the core site in the Cedar Key salt marsh. Inset map shows an outline of the state of Florida, with the study area indicated by a box. **B** Main geomorphological units around the core site (red triangle) **C** picture of the core and surrounding landscape **D** Schematic representation of the profile A-A' (Fig. 1B) showing the relative altitude between high marsh, low marsh and tidal

creek, frequency of flooding and type of vegetation. The altitude between the three environments was approximated with Google Earth Pro. Different environments were defined using elevation profiles, analysis of historical images through recognition of different altitude cover by tidal floods, and changes in the image texture associated with vegetation cover. Because altitude measurement is inaccurate, we simply used relative altitude

Florida. To achieve that, we collected a sediment core and: 1) used ²¹⁰Pb dating to determine the rate of sediment accumulation at the study site, 2) employed stable carbon isotopes (δ¹³C) to assess whether the community of higher plants at the site had changed in response to recent sea-level rise, and 3) evaluated sea-level changes and paleoenvironmental responses, utilizing temporal shifts in the salinity and life-form preferences of sedimented diatom assemblages.

Study area

Our study site is located in the southern portion of the Suwannee River Estuary, within the Big Bend region of Florida’s Gulf of Mexico coast (Fig. 1). The Big Bend is a low-gradient, low-wave-energy coastline that supports vast expanses of salt marsh, with coastal forest farther inland and in elevated

patches throughout the marsh (Hine et al. 1988). Much of this coastline is held as federal, state, or local protected land. Most of the Suwannee Estuary’s wetlands and forests are preserved as part of the Lower Suwannee National Wildlife Refuge, though the coring site is just outside the Refuge boundary. The region has a low amount of impervious surface and little industrial or residential development, with high coverage of wetlands and upland forests (Seavey et al. 2011). The region has a warm, sub-tropical climate that is characterized by long, wet summers (Mattson et al. 2007).

The region’s coastal wetlands began forming during the Middle Holocene, when sea-level rise drowned Pleistocene dunes, forming offshore sandy shoals. Then, during the Middle to Late Holocene highstand, the coast became aggradational, as fluvial input increased and the shoreline stabilized.

The modern marsh system formed in the Late Holocene (Wright et al. 2005). The region is underlain by shallow limestone bedrock with karstic features, which leads to rapid and spatially irregular surface–groundwater exchange (Mattson et al. 2007). Dissolution of this underlying bedrock led to development of an irregular topography that influences modern ecosystem distributions and sedimentation patterns (Hine et al. 1988).

Materials and methods

On 16 January 2015, we collected an 84-cm-long sediment core from a site (N 29° 14' 57.0", W 83° 03' 05.1") that lies ~15 m from a tidal creek in a high salt marsh, where the marsh surface is just above mean sea-level and experiences low-frequency tidal inundation (Fig. 1). The core was taken with a sediment–water interface corer (Fisher et al. 1992), ~10 km north of the town of Cedar Key, and at a roughly equivalent distance southeast of the mouth of the Suwannee River. We selected the sampling site in the high salt-marsh environment with the objective of documenting the Late Holocene transgression, and to test whether there had been a transition from a freshwater wetland or Holocene intertidal zone to a salt-marsh environment. Previous studies south of the Suwannee River (Wright et al. 2005) showed that the salt-marsh facies accumulated after the Late Holocene transgression. Thereafter, the Eocene limestones were covered with ~1.2 m of sediment at the shoreline, with decreasing thicknesses farther inland. Vegetation at the core site is dominated by the rush *Juncus roemerianus*, whereas nearby areas, particularly along the tidal creek edges, host cordgrass (*Spartina alterniflora*). The retrieved core was maintained in a vertical position and extruded and sampled in the field at 4-cm intervals. Samples were placed in labeled containers and transported to the laboratory where they were refrigerated at 4 °C prior to analysis.

Bulk density and core chronology

Bulk density (dry mass cm⁻³ wet) in each stratigraphic sample was determined by weighing a measured volume of wet sediment, freeze-drying, and re-weighing. Age–depth relations for the salt-marsh-sediment core were determined by ²¹⁰Pb dating. We

used EG&G Ortec, low-background, well-type germanium detectors, connected to a 4096-channel, multi-channel analyzer, to measure total and supported ²¹⁰Pb activities (Appleby et al. 1986; Schelske et al. 1994). Total ²¹⁰Pb activity was obtained from the photopeak at 46.5 keV. Radium-226 activity (i.e., supported ²¹⁰Pb activity) was estimated by averaging the activities of ²¹⁴Pb (295.1 keV), ²¹⁴Pb (351.9 keV), and ²¹⁴Bi (609.3 keV; Moore 1984). Unsupported (excess) ²¹⁰Pb activity in each sample was determined by subtracting ²²⁶Ra activity (i.e., supported ²¹⁰Pb activity) from total ²¹⁰Pb activity. We calculated sediment ages with the constant-flux, constant-sedimentation (CFCS) model (Krishnaswamy et al. 1971). We estimated the average mass-sedimentation rate (MSR, mg cm⁻² a⁻¹) as the quotient of the decay constant of ²¹⁰Pb (0.031) divided by the slope of the regression of the natural log of unsupported ²¹⁰Pb against the mid-depth cumulative mass (mg cm⁻²). We calculated age errors using the 95% confidence interval of that MSR estimate. Cesium-137 activity was determined simultaneously from the 661.7 keV photopeak, in an effort to identify the 1963 cesium fallout maximum caused by atmospheric bomb testing (Krishnaswami and Lal 1978). Dates on sediment depths below the unsupported/supported ²¹⁰Pb boundary were estimated by downward extrapolation of the average MSR calculated for the datable, topmost 24 cm of the core.

Sediment geochemistry

The total organic carbon to nitrogen ratio (TOC/TN) and δ¹³C values of sediment organic matter (OM) are commonly used to identify the source of sediment OM (algae/macrophytes vs terrestrial plants) and the photosynthetic pathway (C3 and C4) used by the vegetation that contributed to that OM, respectively (Lamb et al. 2006). We calculated the TOC/TN ratio to distinguish algal-dominated tidal flats from salt-marsh environments inhabited by emergent higher plants. We used the δ¹³C of the OM to recognize vegetation shifts between C4 *Spartina alterniflora*, which dominates in low salt-marsh environments to C3 *Juncus roemerianus*, which is more abundant in high salt-marsh areas. In addition, total nitrogen (TN) and δ¹⁵N analyses enabled us to identify periods of greater algal contribution to the sediment and early diagenesis (Yu et al. 2018).

OM content in dry sediment was measured by weight loss on ignition for 2 h at 550 °C. Total carbon (TC) and TN were determined using a Carlo-Erba NA 1500 C/N/S analyzer. Total inorganic (carbonate) carbon (TIC) was measured by coulometry (Englemann et al. 1985). Weight percent of the carbonate component of the sediment was calculated as $8.333 \times \text{TIC}$ (%), assuming that all inorganic carbon is bound in CaCO_3 . TOC was calculated as TC minus TIC, and the carbon/nitrogen ratio was figured as % mass TOC/% mass TN.

The $\delta^{13}\text{C}$ values of sediment TOC were measured after decarbonation by acidification with 1 N HCl and rinsing with de-ionized water. Stable isotopes of nitrogen ($\delta^{15}\text{N}$) in OM were run on bulk dry, non-acidified sediment. Samples for stable isotope analyses were loaded into tin capsules that were placed in a carousel atop a Carlo Erba NA1500 elemental analyzer. After flash combustion in a quartz column at 1000 °C in an oxygen-rich atmosphere, generated gas entered a He carrier stream and passed through a hot elemental Cu reduction column (650 °C) to remove oxygen. Water was removed from the gas when it passed through a magnesium perchlorate trap. The effluent stream from the elemental analyzer was connected to a Thermo Electron DeltaV Advantage isotope ratio mass spectrometer via a Thermo Finnigan ConFlo II interface. Carbon and nitrogen isotope results were measured relative to an internal laboratory-reference standard and calibrated to Vienna Pee Dee Belemnite (VPDB) and Air, respectively. Isotope ratios are expressed as permil in standard delta notation. The lithologic and geochemical diagrams were made with the *tidypaleo* package (Dunnington et al. 2022) for R software (R Core Team 2020) and the zonation of the core was achieved using a constrained hierarchical cluster analysis with CONISS, using the *Rioja* package (Juggins 2017).

Diatoms

We selected diatoms as environmental bioindicators for this study because they: 1) were numerous and well-preserved in most samples throughout the sediment core, 2) have well-established and distinct ecological preferences, and 3) respond rapidly to environmental changes. These characteristics made them ideal microfossils for inferring past shifts in

salinity and tidal exposure, and therefore past sea-level change (Vos and de Wolf 1993; Taffs et al. 2017).

Subsamples for diatom analysis were prepared from every 4-cm sediment interval, using standard protocols (Battarbee et al. 2001). Briefly, 0.1–0.2 g of sediment that had been dried at room temperature, was placed in 30 mL of 30% H_2O_2 for 48 h to remove OM. Digested samples were rinsed with distilled water and centrifuged three times and brought to a final volume of 40 mL. Using a disposable pipette, 0.3 μL was removed, placed on a cover slip, and dried at room temperature. Permanent slides were mounted in Zrax (RI- 1.7+) and previewed to ensure diatom density was not excessive. Samples from depths of 8, 28, 60, 64, and 72 cm were too dense, and therefore diluted to a volume of 80 mL. Diatoms were identified and counted at 1000 \times magnification with an Olympus CX31 microscope. At least 400 diatom frustules were counted per slide. Diatoms were identified to the lowest taxonomic level when possible, using the Diatoms of North America online database (diatoms.org; Spaulding et al. 2022) and Witkowski et al. (2000). Valve preservation in samples from the core was noted. Absolute diatom counts were transformed to relative counts using *Tilia* and plotted with *Tiliagraph* software version 2.6.1. (Grimm 1992). Species with <2% abundance were not included in the analysis, except if they were present in at least three consecutive samples.

Ecological information for each species came from a variety of sources, with the main references being Denys (1991), Vos and de Wolf (1993) and Witkowski et al. (2000). To infer the past environmental conditions at the core site, diatoms were grouped based on lifeform (planktonic, benthic, epiphytic, tychoplanktonic) and salinity (freshwater, freshwater-brackish, slightly freshwater-brackish, brackish-marine, marine-brackish) preferences (Vos and de Wolf 1993; Table 1). Salinity ranges for the marine, estuarine (brackish) and freshwater environments are 20–35, 5–20 and 0–5 psu, respectively (Parsons 1998; based on Round 1981). Qualitative observations on the appearance of non-opaque iron hydroxides (hematite/limonite) in the diatom slides were used to distinguish subaqueous from exposed conditions, assuming oxidation occurred under subaerial conditions.

Table 1 Ecology of diatoms recorded in the Cedar Key sediment core (See additional information in ESM)

Species	Salinity	Lifeform	Figures on ESM
<i>Cocconeis cascadiensis</i>	Freshwater ¹⁰	Benthic ¹⁰	Fig. S11
<i>Cyclotella distinguenda</i>	Freshwater ¹¹	Planktonic ¹¹	Fig. S15
<i>Diploneis calcilacustris</i>	Freshwater ¹²	Benthic ¹²	Fig. S10
<i>Diploneis weissflogii</i>	Marine ¹	Benthic epipelagic ²	Fig. S7
<i>Hyalodiscus scoticus</i>	Marine brackish – Brackish marine ¹	Tycho planktonic ¹ ; epiphytic ²	Fig. S5
<i>Nitzschia granulata</i>	Marine brackish – Brackish marine ¹	Benthic epipelagic ²	Fig. S6
<i>Paralia sulcata</i>	Brackish marine ⁴	Tycho planktonic ¹⁴	Fig. S3 and S4
<i>Paralia sulcata</i> var. <i>genuina</i> f. <i>coronata</i>	Marine ⁵		Fig. S1
<i>Paralia sulcata</i> var. <i>genuina</i> f. <i>radiata</i>	Marine ⁵	Tycho planktonic; epiphytic ⁶	Fig. S2
<i>Pseudopodosira echinus</i>	Marine – brackish ¹³	Benthic ¹³	Fig. S8 and S9
<i>Thalassiosira cedarkeyensis</i>	Marine ⁷	Benthic ⁷	Fig. S12
<i>Achnanthes taylorensis</i>	Freshwater ¹⁷		Fig. S16
<i>Actinopterychus</i> cf. <i>splendens</i>	Marine ²	Plankton ²	Fig. S17
<i>Actinopterychus senarius</i>	Marine ³		Fig. S18
<i>Cosmioneis brasiliana</i>	Fresh – Brackish ⁸		Fig. S14
<i>Grammatophora</i> cf. <i>oceanica</i>	Marine ²	Plankton; epiphytic ²	Fig. S19
<i>Planothidium</i> cf. <i>delicatulum</i>	Brackish ¹⁵		Fig. S20 and S21
<i>Staurosirella martyi</i>	Slightly freshwater – brackish ¹⁴	Benthic	Fig. S22
<i>Thalassiosira eccentrica</i>	Marine ²	Plankton ²	Fig. S23
<i>Tryblionella compressa</i>	Marine brackish ¹⁶		Fig. S24
<i>Tryblionella hyalina</i>	Marine brackish – brackish marine ⁹	Benthic ⁹	Fig. S13

(1) Denys (1991); (2) Vos and de Wolf (1993); (3) Witkowski et al. (2000); (4) McQuoid and Nordberg (2002); (5) Sims and Crawford (2017); (6) Siqueiros Beltrones and López Fuerte (2003); (7) Costa-Böddeker et al. (2017); (8) Wetzel et al. (2017); (9) Mandal et al. (2020); (10) Stancheva (2019); (11) Lowe and Manoylov (2011); (12) Jovanovska et al. (2019); (13) Bergamino et al. (2018); (14) Pedraza Garzon (2014); (15) Riaux-Gobin et al. (2018); (16) Bertolli et al. (2020); (17) Antarctic Freshwater Diatoms (2010)

We used relative abundance of sponge spicules as an additional indicator of marine influence.

Samples were normalized by square root transformation to compensate for large differences in abundance between rare and abundant species (Legendre and Gallagher 2001), using the Vegan package (Oksanen et al. 2019) from R software (R Core Team 2020). Diatom zones were defined using a constrained hierarchical cluster analysis with CONISS, using the Rioja package (Juggins 2017). Reported depths for diatom zones are the sample mid-points.

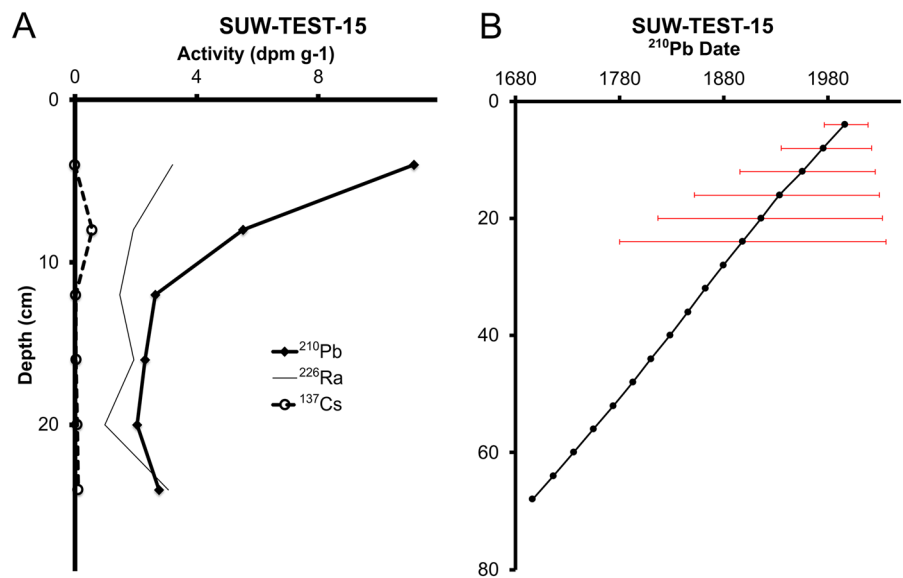
Results

Core chronology

Total ²¹⁰Pb activity in the uppermost 24 cm of the core ranged from a high of 11.1 to a low of 2.0

dpm g⁻¹ (Fig. 2). Supported ²¹⁰Pb activity (²²⁶Ra) was generally low, between 1.0 and 3.2 dpm g⁻¹. Unsupported ²¹⁰Pb activity in the profile declined relatively consistently from a maximum of 8.2 dpm g⁻¹ in the topmost section (0–4 cm) to 1.1 dpm g⁻¹ in the 16–20 cm section, and then to zero (i.e., supported ²¹⁰Pb only) in the 20–24 cm interval (Fig. 2). The oldest calculated ²¹⁰Pb date, at 24 cm, was CE 1898 (Fig. 2), indicating that 24 cm of sediment had accumulated in the last ~120 years. The cumulative excess ²¹⁰Pb inventory at the core site was 15.2 dpm cm⁻². The linear sedimentation rate in the ²¹⁰Pb-datable section of the core was nearly constant, with each 4-cm interval representing accumulation over a period of 17.7–21.7 years. We used the relatively constant MSR measured in the topmost 24 cm (54.7 mg cm⁻² a⁻¹ [~2.1 mm a⁻¹]) to extrapolate age-depth relationships downward, and calculated an estimated age of ~320 years (ca. 1700 CE) at 68 cm in the core, the depth over

Fig. 2 **A** Total ^{210}Pb , ^{226}Ra (supported ^{210}Pb) and ^{137}Cs activities versus depth in the Cedar Key salt-marsh core. **B** Date versus depth in the Cedar Key salt-marsh core. Solid circles indicate dates derived from the CFCS ^{210}Pb dating model. Red error bars show uncertainties (95% confidence intervals) for the dates. The date/depth line below ~ 1900 CE was extrapolated to 68 cm, using the mean mass sediment accumulation rate of $54.7 \text{ mg cm}^{-2} \text{ a}^{-1}$ ($\sim 0.21 \text{ cm a}^{-1}$) from the datable, upper part of the section



which sediment-bulk density remained nearly constant. The only sample with a slight peak in ^{137}Cs activity came from 4–8 cm depth (Fig. 2), but yielded an activity of only 0.6 dpm g^{-1} . The bottommost two samples each displayed barely detectable ^{137}Cs activity values of 0.1 dpm g^{-1} , whereas other levels in the core were entirely devoid of ^{137}Cs activity.

Sediment composition and stable isotopes

Sediments in the three basal samples (84–72 cm) had relatively high bulk densities, between 0.695 and $0.778 \text{ g dry cm}^{-3}$ wet, and were far denser than overlying deposits and much lighter in appearance. The bottom four samples (84–68 cm) had TIC values between 6.0 and 10.0% (Fig. 3), indicating they were composed of ~50.3–83.5% CaCO_3 . The interval from 72 to 68 cm marks a transition to somewhat less dense ($0.469 \text{ g dry cm}^{-3}$ wet) and less mineral-rich deposits. Above 68 cm, bulk density of the sediments varied little, ranging from a low of $0.231 \text{ g dry cm}^{-3}$ wet at 36–32 cm, to a high of $0.297 \text{ g dry cm}^{-3}$ wet at 16–12 cm (Fig. 3).

OM content in the carbonate-rich sediments in the bottom sections was relatively low, ranging from 6.5 to 15.4%. OM content in the uppermost 68 cm ranged from a low of 29.4% in surface deposits (4–0 cm) to a high of 42.2% in sediments at 20–16 cm (Fig. 3). TOC content in the uppermost 68 cm varied from

a low of 11.8% at 16–12 cm, to a high of 19.1% at 20–16 cm (Fig. 3). TOC represented a fairly constant proportion of OM (44–53%). The TOC/TN weight ratios in the core remained relatively constant throughout, generally ranging between 17.1 (8–4 cm) and 21.1 (56–52 cm; Fig. 3). A peak TOC/TN value of 25.1, however, was registered at 72–68 cm, and the lowest value, 13.7, was measured in the topmost sample (4–0 cm).

The lowest $\delta^{13}\text{C}$ values were recorded in the basal four samples and ranged from -27.18 to -26.61‰ (Fig. 3). Throughout the uppermost 68 cm of the core, $\delta^{13}\text{C}$ ranged between a low of -26.36‰ (68–64 cm) and a high of -24.44‰ (56–52 cm). Nitrogen isotope values ranged from a low of 1.09‰ (48–44 cm) to a high of 2.50‰ (12–8 cm) between 84 and 8 cm, but showed slightly higher values in the topmost two samples, 3.24‰ (8–4 cm) and 4.67‰ (4–0 cm; Fig. 3). Cluster analysis on the lithologic and geochemical variables identified three zones in the core: zone 1 (84–68 cm), zone 2 (68–16 cm), and zone 3 (16–0 cm).

Diatoms

Cluster analysis identified four main diatom zones (Fig. 4). The sample from 84–80 cm had insufficient diatoms to achieve minimum counts and was excluded from zonal analysis. Basal samples contained sponge spicules and abundant carbonate.

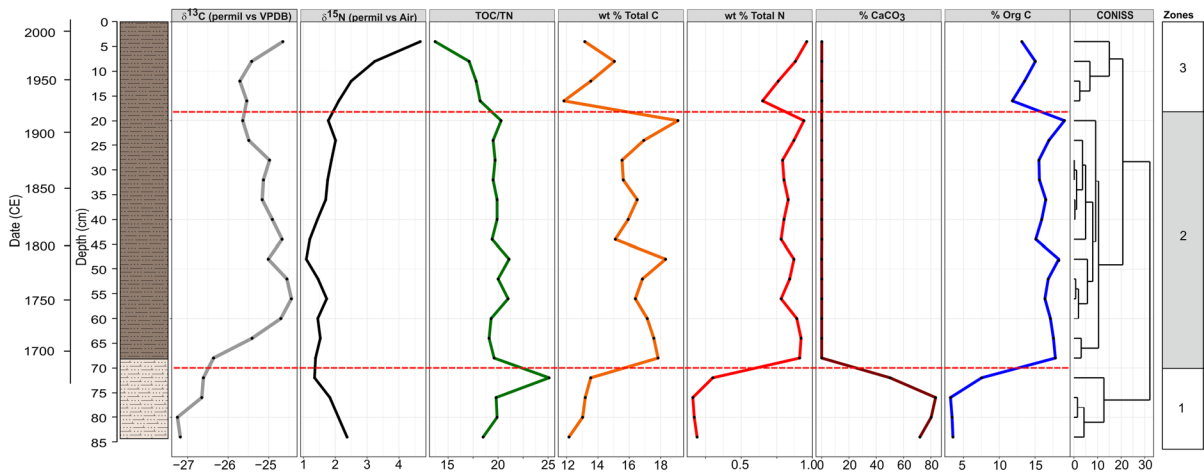


Fig. 3 Stratigraphic section of the Cedar Key core versus depth and date along with carbon and nitrogen stable isotope values ($\delta^{13}\text{C}$ and $\delta^{15}\text{N}$) in OM, the total organic carbon to total

nitrogen ratio (TOC/TN), total carbon (TC), total nitrogen (TN), percent calcium carbonate ($\% \text{CaCO}_3$), percent organic matter ($\% \text{org C}$), and geochemistry zones

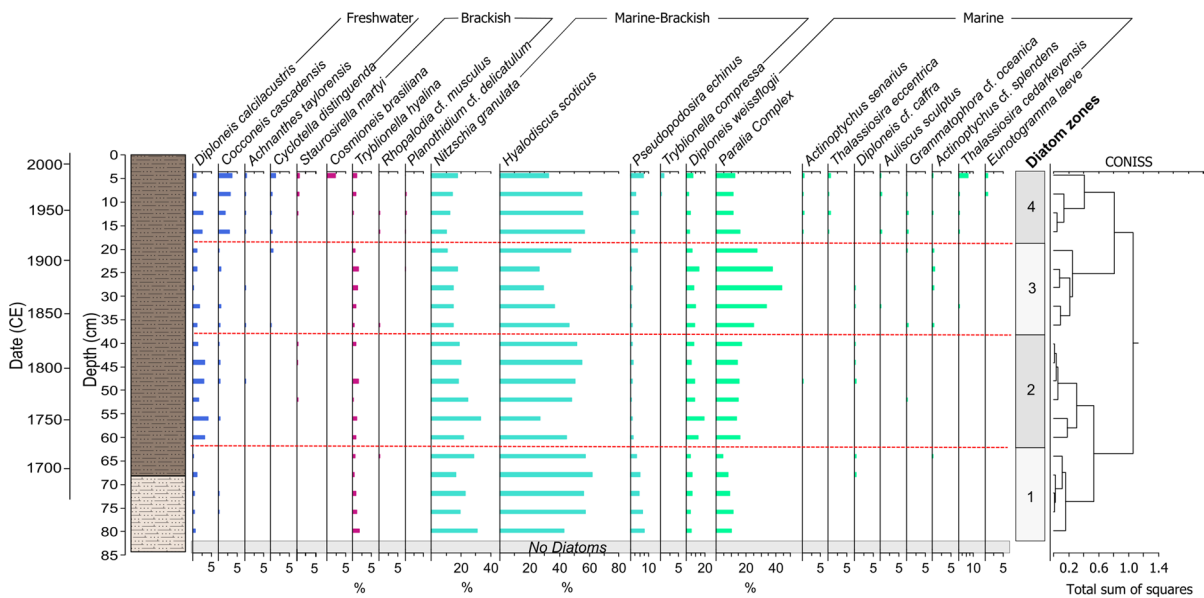


Fig. 4 Stratigraphic section of the Cedar Key versus depth (cm) and date (CE) with relative abundances of diatom taxa grouped by salinity preference and diatoms zones based on CONISS analysis

Several varieties of *Paralia sulcata* were identified in the core, including *Paralia sulcata* var. *genuina* f. *coronata* (Ehrenberg) Grunow (Electronic Supplementary Material [ESM] Fig. S1), *Paralia sulcata* var. *genuina* f. *radiata* (Grunow) (ESM Fig. S2), and *Paralia sulcata* (Ehrenberg) Cleve (ESM Figs. S3 and 4). Because all three have similar ecologies

and relative distributions throughout the core, they were grouped under “*Paralia* complex”.

Diatom zones

Zone 1 (82–62 cm, pre-1700 to ~1720 CE): Frustules of freshwater species in this zone are commonly fragmented or dissolved, whereas those of marine

and brackish-marine species are relatively intact. Iron hydroxides are abundant from 80 to 72 cm, and sponge spicules are rare throughout the zone. The zone is dominated by the marine-brackish diatoms *Hyalodiscus scoticus* Kutzling (mean=58%; maximum=62% at 68 cm; ESM Fig. S5) and *Nitzschia granulata* Grunow (mean=22%; maximum=29% at 64 cm; ESM Fig. S6). This zone contains moderate amounts of marine species *Diploneis weissflogii* (A.W.F. Schmidt) (mean=5%; ESM Fig. S7), *Paralia* complex (mean=8%) and marine brackish *Pseudopodosira echinus* (Frenguelli) (mean=5%; ESM Fig. S8 and S9), which decrease in relative abundance toward the top of the interval. Benthic freshwater species *Diploneis calcilacustris* Lange-Bertalot and A. Fuhrmann (ESM Fig. S10) first appears at 80 cm and thereafter has a mean relative abundance of ~0.63%, with a maximum at 1.15% at 68 cm. Freshwater *Cocconeis cascadenis* Stancheva (ESM Fig. S11) was encountered at 76 and 72 cm at abundances near 1%.

Zone 2 (62–34 cm, ~1720–1830 CE): Freshwater taxa at 60 and 36 cm are fragmented, but are relatively intact from 52 to 40 cm. Marine-brackish species *N. granulata* is fragmented in the interval 48–44 cm. Iron hydroxide abundance is low, while sponge-spicule abundance is moderate. As in Zone 1, this zone is co-dominated by *H. scoticus* (mean=46%; maximum=55% at 44 cm) and *N. granulata* (mean=22%; maximum=33% at 56 cm). Where *N. granulata* is at its highest (56 cm), *H. scoticus* is at its lowest (27%). Also present are moderate amounts of *D. weissflogii* (mean=10%; maximum=19% at 56 cm) and *Paralia* complex (mean=17%; maximum=25% at 36 cm). Diatoms of the *Paralia* complex have their lowest relative abundance (14%) at 56 cm, whereas *D. weissflogii* has its lowest abundance (5%) at 44 cm. This interval also marks the appearance of the marine benthic species *Thalassiosira cedarkeyensis* (A.K.S.K. Prasad) (ESM Fig. S12), but only at 36 cm. There is an increase in freshwater species compared to the previous zone, mostly represented by *D. calcilacustris* and *C. cascadenis*. Also present in low relative abundances are *P. echinus* and the benthic, marine brackish species *Tryblionella hyalina* (Amosse) (ESM Fig. S13).

Zone 3 (34–18 cm, ~1830–1930 CE): The zone has abundant diatom fragments and moderate amounts of sponge spicules. At 24 cm, sponge spicules increase in abundance, and when observed, freshwater species

are intact. Low to moderate iron hydroxides. Mean relative abundance of marine-brackish *H. scoticus* falls slightly in this zone (mean=35%; maximum=48% at 20 cm), whereas that of marine *Paralia* complex (mean=36%; maximum=44% at 28 cm) and *D. weissflogii* (mean=9.5%; maximum=18% at 24 cm) increases. *Nitzschia granulata* relative abundance declines somewhat in the zone (mean=15%) and remains low throughout. The abundance of freshwater species *C. cascadenis* and *C. distinguenda* decrease compared to the previous zone.

Zone 4 (18–2 cm, 1930–2015): This zone contains abundant diatom fragments, but freshwater species are intact. Iron hydroxide abundance is low to absent, while sponge-spicule abundance is moderate. The zone is dominated by marine-brackish *H. scoticus* (mean=50%; maximum=57% at 16 cm), *P. echinus*, and *N. granulata* (mean=14%; maximum=18% at 4 cm). The marine *T. cedarkeyensis* reappears and increases in abundance abruptly at 4 cm. Abundance of the marine *Paralia* complex (mean=13%; maximum=16% at 16 cm) decreases compared to the previous zone. Abundances of freshwater species *C. cascadenis* and *C. distinguenda* increase towards the top of the zone, whereas *D. calcilacustris* decreases. The fresh- to brackish-water diatom *Cosmionella brasiliensis* (Cleve) appears at 4 cm (ESM Fig. S14).

Discussion

Sediment accumulation

The shift from carbonate-rich sediments to more organic-rich deposits above the base of our Cedar Key core was concordant with previous sediment stratigraphic descriptions from the area and suggested we had captured the entire record of sediment accumulation since the Late Holocene transgression. The ^{210}Pb chronology for the core indicates a relatively constant linear sedimentation rate, ~2.1 mm a^{-1} , from the beginning of the twentieth century until the date of core collection in 2015 (Fig. 2). The integrated, unsupported ^{210}Pb at the site (15.2 dpm cm^{-2}) translates to a fallout rate of 0.47 dpm $\text{cm}^{-2} \text{a}^{-1}$, only slightly less than the mean value of 0.56 dpm $\text{cm}^{-2} \text{a}^{-1}$ recorded for 10 cores taken in Florida's inland Blue Cypress Marsh (Brenner et al. 2001). The integrated excess ^{210}Pb value in the saltmarsh is about

half what is typically reported for cores from Florida lakes, but measures derived from lake-sediment profiles are probably consistently biased toward high values, in that such cores are often deliberately collected from areas of preferential accumulation (i.e., high sedimentation rate), to achieve high temporal sampling resolution. Such areas likely receive resuspended and redeposited sediment that carries with it adsorbed, unsupported ^{210}Pb .

The very low ^{137}Cs “peak” (0.6 dpm g^{-1}) in the 8–4 cm interval occurs in sediments that were deposited between ~1975 and 1995, according the ^{210}Pb dating model. If the “peak” indeed marks the time of maximum atomic bomb fallout (1963), we would have expected it to appear in underlying sediments (12–8 cm), deposited from ~1955 to 1975. There are several reasons why we cannot rely on the ^{137}Cs “peak” to support our ^{210}Pb chronology: (1) ^{137}Cs is notoriously poor as a chronological marker in Florida sediments, which lack 2:1-lattice clays and thus do not bind the radionuclide effectively (Brenner et al. 2001); (2) trace amounts of ^{137}Cs were measured at depths well below where it should be found (24–16 cm, pre-1940), suggesting that it is mobile in the saline sediment porewaters, and (3) ^{137}Cs is probably subject to uptake and recycling by plants in the marsh, leading to a disparity between the time of original ^{137}Cs deposition and the age of sediments in which it is found. Drexler et al. (2018) found evidence of in situ migration of ^{137}Cs in several cores from wetland environments in North America. The authors suggested that ^{137}Cs migration in the sediment, along with radionuclide decay and input of ^{137}Cs in surface waters, compromises the reliability of ^{137}Cs dating in some regions, especially in areas that received low deposition of bomb ^{137}Cs . We considered radiocarbon dating the Cedar Key deposits, but several factors dictated against the approach: (1) the marine reservoir effect, (2) high carbonate content in older deposits, and (3) the existence of radiocarbon “plateaus” during the purported time frame of sediment accumulation. Whereas we cannot use alternative radionuclides to confirm our ^{210}Pb chronology, the total integrated unsupported ^{210}Pb value and ^{210}Pb activity-sediment-depth relations are consistent with what has been measured in other Florida wetlands.

The mean linear sediment-accumulation rate for the last century ($\sim 2.1 \text{ mm a}^{-1}$) is at the low end of the ~ 2.1 – 2.4 mm a^{-1} range for sea-level rise around

Florida obtained from tide-gauge data (Mitchum et al. 2017). This suggests that salt-marsh accretion near Cedar Key is just keeping up with, or slightly lagging behind, the most recent rate of sea-level rise. Smoak et al. (2013) studied two cores from mangrove forests of Everglades National Park, Florida, and found overall rates of accretion of 2.5 and 3.6 mm a^{-1} , with storm deposits contributing to even higher values (5.9 and 6.5 mm a^{-1}), all in excess of the rate of sea-level rise measured at Key West. It is not surprising that different wetland environments along Florida’s coast are experiencing different fates in the face of ongoing sea-level rise. Furthermore, changes in wind and current patterns can alter sea level on short time-scales, from years to decades (Mitchum et al. 2017). In addition, numerous factors can affect local sediment-accretion rates, including, among others: 1) local vegetation type, 2) alluvial transport of material from upland to coastal environments, 3) translocation of marine sediments to the nearshore environment, 4) land surface and subaqueous topography, 5) magnitude and frequency of storm events, and 6) human activities in coastal zones, e.g., land clearance, construction, surface and groundwater withdrawals (Morris et al. 2002; Kirwan et al. 2010). This makes it hard to generalize results from one region to another.

Vegetation changes

Lithologic analysis shows that 68 cm of organic-rich deposits (~ 29 – 42% OM) accumulated atop a carbonate-rich basal layer (~ 50 – 83% CaCO_3) at the core site over the last three centuries (Fig. 3). The TOC/TN ratios of the OM, mostly values in the high teens and low 20s, indicate either a mixture of algal and terrestrial sources, or more likely, a predominantly non-woody macrophyte source (Meyers and Terranes 2001). Kemp et al. (2010) reported similar TOC/TN values in marsh-surface sediments in North Carolina, where *Juncus roemerianus* and *Spartina alterniflora* dominate high marsh and low marsh, respectively. The low TOC/TN value (13.7) in the topmost sample from the Cedar Key core may indicate relatively greater contribution of undegraded algal remains.

Relatively low $\delta^{13}\text{C}$ values throughout the core indicate a dominant C3 plant source to OM in the sediment. This suggests that the rush, *Juncus roemerianus*, has probably grown at the site continuously for

the last three centuries, never having been replaced by C4 cordgrass, *Spartina alterniflora*, which today grows nearby. The rather consistent $\delta^{15}\text{N}$ values throughout the core also argue for an unchanging plant community, and the high values near the surface probably reflect a relative lack of diagenesis, and perhaps a larger contribution to the sediment OM from algae.

Diatom-based paleoenvironmental and sea-level-change inferences

Period 1, pre-1700 to ~1720 CE (82–62 cm)

During this period, a supratidal environment with frequent desiccation prevailed. This is inferred from a diatom assemblage dominated by the marine-brackish and benthic *H. scoticus* (epiphytic), *N. granulata* (epipelagic) and *P. echinus*, which suggest a low-energy, periodically desiccated environment with macrophytes (Vos and Wolf 1993; Fig. 5). Also, the mixture of ecological groups with different life forms (Fig. 4), presence of the tychoplanktonic *P. sulcata*, and the moderate to high presence of iron hydroxides (Fig. 5), suggest very shallow pond conditions, with frequent desiccation in the supratidal environment (Vos and Wolf 1993). *Pseudopodosira echinus* prefers stagnant and eutrophic waters and tolerates a wide range of salinity (optimum 20 psu; Bergamino et al. 2018). It has been used as a reliable indicator of sea-level change, being more abundant during transgressive events (Tanimura and Sato 1997; García-Rodríguez and Witkowski 2003). The near absence of diatoms between 84 and 80 cm, with presence of only a few well silicified diatoms in carbonate-rich sediment (~50–80% CaCO_3), reflects poor frustule preservation. In laboratory experiments and lake sediment samples, Hassan et al. (2020) found that high alkalinity and salinity affected diatom preservation, causing dissolution of poorly silicified taxa.

Period 2, ~1720–1830 CE (68–34 cm)

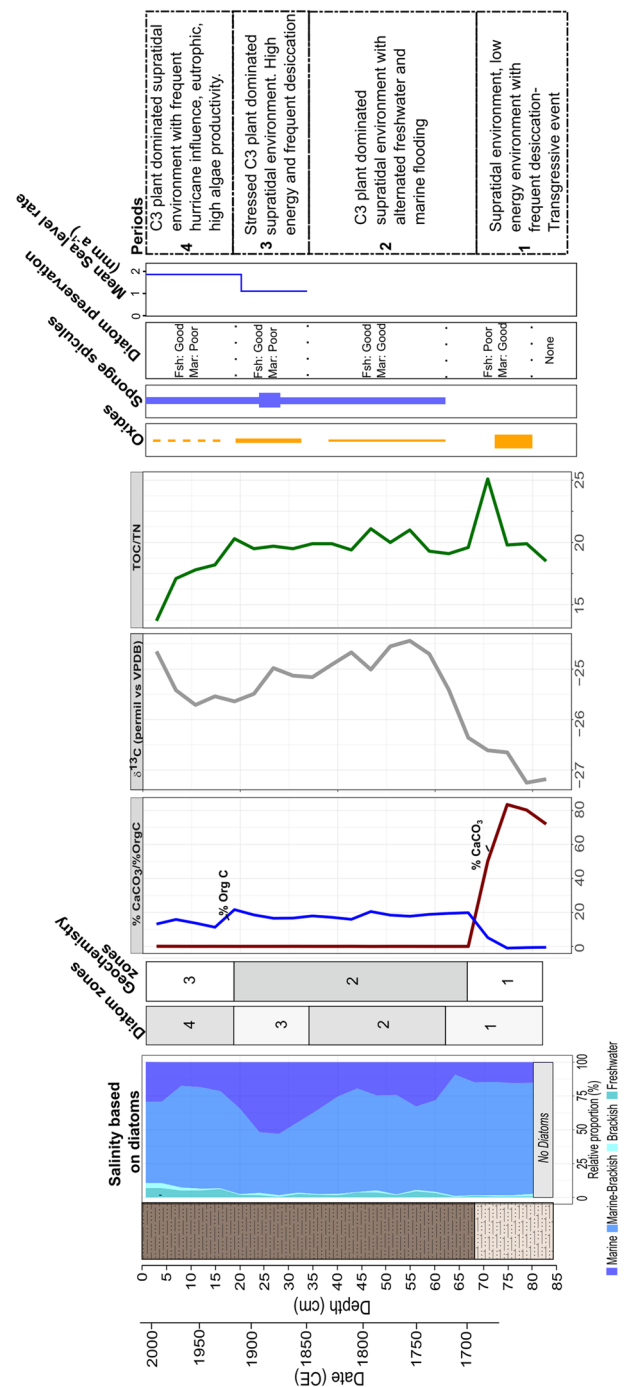
Marine-brackish epiphytic and epipelagic species are still dominant, as in the previous zone, suggesting a low-energy, periodically desiccated environment with macrophytes in the supratidal environment (Vos and Wolf 1993; Fig. 5). Nevertheless, increases of well-preserved benthic freshwater *D. calcilacustris*

and *C. cascadiensis* and the marine species *Paralia* complex and *D. weissflogii*, in addition to increases in sponge spicules and decreases in iron hydroxides, suggests less frequent subaerial exposure and more frequent flooding from both fresh and marine water (Fig. 5). Wilson et al. (2015) found that groundwater controls the vegetation zones. Zones dominated by *Juncus* were characterized by a regularly inundated marsh during spring tides and exposed during periods of sustained upward flow of freshwater during neap tides. Thus, a change in the hydrologic pattern and a slightly higher rate of aggradation than sea-level rise could have favored the establishment of *Juncus roemerianus*. On the other hand, we inferred a decrease in trophic state, expressed as a decrease in *P. echinus* and increase in species that prefer meso-oligotrophic environments (*P. sulcata*, *D. calcilacustris* and *C. cascadiensis*). Lower productivity could be associated with a greater contribution of marine water. Larger contributions of marine water are supported by a slight increase in $\delta^{13}\text{C}$ values, from values between -27.20 and -25.41‰ (84–64 cm) to values from -25.01 to -24.40‰ (62–40 cm; Fig. 5). This may reflect a relative increase in the contribution to OM from *Spartina alterniflora* (C4) versus *Juncus roemerianus* (C3), but might also be a consequence of a shift to a greater relative contribution of marine (-23 to -16‰) versus freshwater algae (-30 to -26‰; Meyers 2001).

Period 3, ~1830–1930 CE (Zone 3; 34–18 cm)

A salt marsh environment with brackish water is inferred from the diatom assemblage. However, brief periods of higher sea-level occurred, as indicated by the increase in marine taxa *Diploneis weissflogii* and *Paralia* complex, the appearance of new marine species, and a moderate amount of sponge spicules (Fig. 5). Frequency of iron hydroxides is low to moderate, likely from increasingly infrequent subaerial exposure, resulting from rising sea-level. Sea level rose from 1850 to 1914 at a rate of ~1.1 mm a^{-1} (Raabe and Stumpf 2016; Fig. 5). Sea-level rise may also account for the decline in *H. scoticus* relative abundance, as it normally grows attached to plants, and if sea level rises too rapidly, salt-marsh plants drown or become stressed by frequent salinity shifts. Tide-gauge records from Cedar Key acquired since 1914 show a mean sea-level increase of ~1.8 mm

Fig. 5 Paleoenvironmental interpretation of the Cedar Key record showing stratigraphic section, salinity changes inferred from diatoms, diatom and geochemistry zones based on cluster analysis, percentage CaCO_3 and TOC, $\delta^{13}\text{C}$, TOC/TN ratio, relative preservation of iron hydroxides and sponge spicules (bar width is proportional to the abundance, whereas dashes indicate absence or low abundance), diatom preservation, mean rate of sea-level rise (mm a^{-1}) at Cedar Key, based on Raabe and Stumpf (2016) and identified periods of salt-marsh evolution. Fsh: Freshwater and Mar: Marine



a^{-1} (Raabe and Stumpf 2016; Fig. 5). Salinity conditions during this zone are inferred to reflect a marine-brackish salt marsh. A larger tidal range may have been responsible for greater energy of the environment, supported by an increase in the tycho planktonic *Paralia* complex and diatom fragmentation.

Period 4, ~1930–2015 CE (Zone 4; 18–2 cm)

Dominance of marine-brackish epiphytic and epipelagic species, mainly *H. scoticus*, *N. granulata* and *P. echinus* suggests that salt-marsh conditions continued to prevail. An increase in hurricane influence is

suggested by the higher proportion of fragmented individuals (high energy), an increase in species number and diversity of all the salinity groups, and a decrease in TOC (Fig. 5). Mixed assemblages, composed of freshwater, brackish and marine diatoms, have been described as a characteristic of tsunami deposits (Dawson et al. 1996; Dawson 2007; Kokociński et al. 2009; Wang et al. 2019). The National Hurricane Center recorded more than 20 hurricanes that crossed the Gulf of Mexico or Florida coast since 1900 (<https://www.nhc.noaa.gov/outreach/history/>). The 1933 Atlantic hurricane season was one of the most active on record, with 20 storms (Klotzbach et al. 2021). Consequent high river discharge may account for the increase in freshwater diatoms. Higher precipitation is suggested by an increase in freshwater diatom species and the first appearance of *C. brasiliensis*. Although mean annual rainfall did not change significantly from 1941 to 2008, the Suwannee River discharged large pulses of freshwater during the spring months and after tropical storms of late summer and early fall (Seavey et al. 2011). The appearance of *T. cedarkeyensis*, which prefers brackish water and high nutrient concentrations, suggests an increase in trophic state conditions (Castillo 2015). Higher nutrient concentrations probably also caused the increase in epiphytic *H. scoticus* and the relative increase in algal-derived OM, as indicated by lower TOC/TN (Fig. 5). Sediment resuspension and mixing of marine and fresh waters under high-energy conditions are inferred from the increase in benthic *P. echinus* (Bergamino et al. 2018).

Between 1941 and 2011, the average high water (MHHW) at Cedar Key increased approximately 0.2 m with a relative sea-level-rise rate of $2.19 \pm 0.18 \text{ mm a}^{-1}$ (NOAA 2019). Sea-level has not increased monotonically on the Florida Gulf Coast. Rather, periods of rapid rise in sea-level are followed by periods of stable or even falling sea-level (Raabe and Stumpf 2016). An increase in storm frequency during Period 4 may have provided a greater supply of sediment from the nearshore environment to the salt marsh, favoring a rate of aggradation that exceeded the rate of sea-level rise. Several salt marshes with a limited sediment supply, like those of the Florida Big Bend region (Coultas and Hsieh 1997), and others in Connecticut, Virginia, and the Arctic (Tiner 2013) have benefited from higher episodic deposition during periods of greater hurricane activity.

Resilience of Big Bend region to sea-level rise

Our “paleo” data support previous findings that indicate rising sea-levels and changing tidal regimes in the area. We found that despite rising sea-level, the salt marsh near Cedar Key has persisted throughout the last ~320 years, likely because aggradation rates have equaled or exceeded rates of sea-level rise. Empirical studies and numerical models show that salt marshes respond to sea-level rise with sediment accretion that maintains the elevation necessary to support marsh plants like *Spartina*, assuming that other stressors remain minimal (Fagherazzi et al. 2012; Kirwan and Megonigal 2013). Despite the low sediment supply in the Cedar Key area, it has been observed that re-suspension of sediments from the nearshore environment and their deposition onto the marsh are facilitated by wind, tropical storms, and high-tide events (Goodbred and Hine 1995; Leonard et al. 1995). Furthermore, coastal protection measures and hydrological stability have favored continuous biotic accommodation and self-regulation processes, which have enabled the salt marsh to keep pace with sea-level rise (Raabe and Stumpf 2016). Nevertheless, sea-level rise has had substantial impacts throughout the Big Bend region, particularly on adjacent coastal forests that have been forced to migrate inland as they have become increasingly exposed to saline water and the salt-marsh environment extends landward. Raabe and Stumpf (2016) found that over a 120-year period, through 1995, the marsh/forest boundary moved inland, while marsh erosion at the coastal edge has been modest, resulting in a net increase of 23% in salt-marsh area. Although this represents a concerning loss of coastal forest habitat, the ability of these salt-marsh ecosystems to accrete and expand as salt-water penetrates farther inland is an encouraging indication of the coastline’s climate resiliency.

Whereas the Big Bend area on Florida’s Gulf Coast is in some ways highly susceptible to sea-level rise, it possesses several characteristics that make it resilient. Because of the low-lying regional topography, vertical changes in mean sea-level have the potential to submerge large areas of salt marsh, as occurred during the period ~1850–1930 CE. Nevertheless, it appears that salt-marsh conditions recovered quickly, as seen in the diatom assemblages thereafter. Although the Big Bend region receives a low sediment supply, which has been shown in other

areas to constrain the ability of salt marsh to accrete (Kirwan and Megonigal 2013), its sediment input is not restricted by anthropogenic barriers, which are present along many other coastlines. The area's low development and vast marsh acreage also create a high degree of contiguity, providing a large seed bank that facilitates marsh migration.

Should the rate of sea-level rise and other climate-change impacts continue to increase, however, we can anticipate transformative changes in salt-marsh communities. It is expected that as air temperature increases and freeze frequency decreases, many salt marshes near Cedar Key will be replaced by mangrove forest (Cavanaugh et al. 2014; Saintilan et al. 2014; Giri and Long 2016). Establishment of mangrove forest might increase resilience in the face of sea-level rise, given that studies in north and south Florida have shown higher sedimentation rates in mangrove forests compared to salt marshes (Smoak et al. 2013; Vaughn et al. 2020). If other anthropogenic stressors are kept to a minimum, and especially if the transition to mangrove forest occurs as expected, there is high potential for coastal wetlands in this area to remain intact.

Conclusions

Approximately 68 cm of relatively organic-rich sediment accumulated atop carbonate-dominated material at the Cedar Key core site during the last ~320 years. The top 24 cm were datable by ^{210}Pb and showed that sediment accumulation was relatively constant since the beginning of the twentieth century, accreting at a mean rate of $54.7 \text{ mg cm}^{-2} \text{ a}^{-1}$ ($\sim 0.21 \text{ cm a}^{-1}$).

Paleoenvironmental inferences suggest a salt-marsh environment dominated by C3 plants, most likely *Juncus roemerianus*, persisted from ~1700 CE to present. This was indicated by intermediate TOC/TN ratios in the sediments (high teens-low 20s), along with relatively low $\delta^{13}\text{C}$ values. Diatoms suggest the salt marsh experienced moderate salinity variations that likely reflect sea-level changes, but may also have been a consequence of variations in freshwater delivery. Between ~1850 and 1930 CE, we observed an increase in salinity (marine incursions), with a probable decline in plant productivity. Nevertheless, the salt-marsh vegetation recovered quickly after 1930 CE, indicating

that the rate of aggradation and vegetation growth kept pace with the rate of sea-level rise. The increase in the rate of vertical accretion and recovery of the vegetation was probably favored by the increase in storm frequency from 1930 to present, which may have provided a greater supply of sediment and nutrients from nearshore and upland sites to the salt marsh, thereby favoring a rate of aggradation greater than that of sea-level rise. The sedimentation rate measured roughly matches the lower end of sea-level-rise rates during the same period, suggesting the marsh elevation has kept pace with sea-level rise, though just barely. Our data support the idea that salt marshes are resilient to sea-level increase, at least under recent past conditions, and that self-regulating biotic and abiotic processes have enabled the salt marsh to keep pace with sea-level rise. This work provides insight into how biotic and abiotic factors responded to sea-level rise at a single site on Florida's Gulf of Mexico coast. The ability of coastal salt-marsh ecosystems to keep pace with sea-level rise involves complex interactions among climate, geomorphology, hydrology, sedimentology and biology. Additional studies are needed to disentangle those interactions and better understand how coastal environments will respond to future climate change and sea-level rise.

Acknowledgements We thank Vic Doig and other scientists at the Lower Suwannee National Wildlife Refuge for transport to the core site and for providing contextual information on the area. Also, we thank Felipe Garcia-Rodriguez, who helped identify *P. echinus* and provided literature on its ecological preferences. Seitz was funded by The Canadian Queen Elizabeth II Diamond Jubilee Scholarship for Advanced Scholars (QES-AS), which is managed through a unique partnership of Universities in Canada, the Rideau Hall Foundation (RHF), Community Foundations of Canada (CFC) and Canadian universities. The QES-AS is made possible with financial support from the International Development Research Centre (IDRC) and Social Sciences and Humanities Research Council (SSHRC). B. Boyarski was funded through University of Regina Undergraduate Research and an NSERC-DG grant to M. Vélez. Support for sediment sampling and dating was provided by the University of Florida Land Use and Environmental Change Institute. We thank two anonymous reviewers for comments that improved this manuscript.

Author contributions CS, WK, BP-B, MB, MV, and KG wrote the main manuscript text. CS prepared Figs. 1, 4 and 5. WK prepared Fig. 2. JE prepared Fig. 3. BP-B prepared Table 1 and ESM. CS, WK, BP-B, JC, MV, KG, JE and MB reviewed and edited the manuscript.

Declarations

Competing interests The authors declare no competing interests.

Conflict of interest The authors declare no competing interests. Co-authors MV, JE and MB are members of the *Journal of Paleolimnology* editorial staff, but played no part in the review process for this article.

References

- Adam P (2016) Salt Marshes. In: Kennish MJ (ed) *Encyclopedia of Estuaries*. Springer, Dordrecht, pp 515–530
- Appleby PG, Nolan PJ, Gifford DW, Godfrey MJ, Oldfield F, Anderson NJ, Battarbee RW (1986) ^{210}Pb dating by low background gamma counting. *Hydrobiologia* 143:21–27
- Barbier EB, Hacker SD, Kennedy C, Koch EW, Stier AC, Silliman BR (2011) The value of estuarine and coastal ecosystem services. *Ecol Monogr* 81:169–193. <https://doi.org/10.1890/10-1510.1>
- Battarbee RW, Jones VJ, Flower RJ, Cameron NG, Bennion H, Carvalho L, Juggins S (2001) Diatoms. In *Tracking environmental change using lake sediments*. Kluwer Academic Publishers, Dordrecht, pp 155–202. http://link.springer.com/10.1007/0-306-47668-1_8
- Bergamino L, Rodríguez-Gallego L, Perez-Parada A, Rodríguez Chialanza M, Amaral V, Perez L, Scarabino F, Lescano C, García-Sposito C, Costa S, Lane CS, Tuduri A, Venturini N, García-Rodríguez F (2018) Autochthonous organic carbon contributions to the sedimentary pool: a multi-analytical approach in Laguna Garzon. *Org Geochem* 125:55–65
- Breithaupt JL, Smoak JM, Smith TJ III, Sanders CJ (2014) Temporal variability of carbon and nutrient burial, sediment accretion, and mass accumulation over the past century in a carbonate platform mangrove forest of the Florida Everglades. *J Geophys Res-Biogeosci* 119:2032–2048
- Brenner M, Schelske CL, Keenan LW (2001) Historical rates of sediment and nutrient accumulation in marshes of the Upper St. Johns River Basin, Florida, USA. *J Paleolimnol* 26:241–257
- Castillo JAA (2015) Morphological description and autecology of *Thalassiosira cedarkeyensis* (Bacillariophyta: Thalassiosirales) in Sontecomapan Lagoon, Veracruz, Mexico. *Cymbella* 1:12–18
- Cavanaugh KC, Kellner JR, Forde AJ, Gruner DS, Parker JD, Rodriguez W, Feller IC (2014) Poleward expansion of mangroves is a threshold response to decreased frequency of extreme cold events. *PNAS* 111:723–727. <https://doi.org/10.1073/pnas.1315800111>
- Cavanaugh KC, Dangremond EM, Doughty CL, Williams AP, Parker JD, Hayes MA, Rodriguez W, Feller IC (2019) Climate-driven regime shifts in a mangrove-salt marsh ecotone over the past 250 years. *PNAS* 116:21602–21608. <https://doi.org/10.1073/pnas.1902181116>
- Costa-Böddeker S, Xuân Thuyên L, Schwarz A, Đức Huy H, Schwab A (2017) Diatom assemblages in surface sediments along nutrient and salinity gradients of Thi Vai Estuary and can gio mangrove forest, Southern Vietnam. *Estuaries Coast* 40:479–492. <https://doi.org/10.1007/s12237-016-0170-5>
- Coultas CL, Hsieh YP (1997) Ecology and management of tidal marshes: a model from the Gulf of Mexico. St. Lucie Press, Delray Beach, FL
- Craft C, Clough J, Ehman J, Joye S, Park R, Pennings S, Guo H, Machmuller M (2009) Forecasting the effects of accelerated sea-level rise on tidal marsh ecosystem services. *Front Ecol Environ* 7:73–78. <https://doi.org/10.1890/070219>
- Dawson S (2007) Diatom biostratigraphy of tsunami deposits: examples from the 1998 Papua New Guinea tsunami. *Sediment Geol* 200:328–335
- Dawson S, Smith DE, Ruffman A, Shi S (1996) The diatom biostratigraphy of tsunami sediments: examples from recent and middle Holocene events. *Phys Chem Earth* 21:87–92
- Denys L (1991) A checklist of the diatoms in the Holocene deposits of the Western Belgian coastal plain with a survey of their apparent ecological requirements, I. Introduction, ecological code and complete list. *Geological Survey of Belgium, Belgium*
- Desantis LRG, Bhotika S, Williams K, Putz FE (2007) Sea level rise and drought interactions accelerate forest decline on the Gulf Coast of Florida, USA. *Glob Change Biol* 13:2349–2360
- Dunnington DW, Libera N, Kurek J, Spooner IS, Gagnon GA (2022) Tidypaleo: Visualizing Paleoenvironmental Archives Using ggplot2. *Journal of Statistical Software* 101(7):1–20. <https://doi.org/10.18637/jss>
- Englemann EE, Jackson LL, Norton DR, et al (1985) Determination of carbonate carbon in geological materials by coulometric titration. *Chem Geol* 53:125–128.
- Fagherazzi S, Kirwan ML, Mudd SM, Guntenspergen GR, Temmerman S, D’Alpaos A, van de Koppel J, Rybczyk JM, Reyes E, Craft C, Clough J (2012) Numerical models of salt marsh evolution: ecological geomorphic and climatic factors. *Rev Geophys* 50:RG1002. <https://doi.org/10.1029/2011RG000359>
- Fisher MM, Brenner M, Reddy KR (1992) A simple, inexpensive piston corer for collecting undisturbed sediment/water interface profiles. *J Paleolimnol* 7:157–161
- Florida department of environmental protection (2020). Salt marshes. <https://floridadep.gov/rcp/saltmarshes>. Accessed 10/29/2020
- García-Rodríguez F, Witkowski A (2003) Inferring sea level variation from relative percentages of *Pseudopodosira kosugii* in Rocha Lagoon, SE Uruguay. *Diatom Res* 18:49–59. <https://doi.org/10.1080/0269249X.2003.9705572>
- Geselbracht L, Freeman K, Kelly E, Gordon DR, Putz FE (2011) Retrospective and prospective model simulations of sea level rise impacts on Gulf of Mexico coastal marshes and forests in Waccasassa Bay, Florida. *Clim Change* 107:35–57
- Giri C, Long J (2016) Is the geographic range of mangrove forests in the conterminous United States really expanding? *Sensors* 16:2010. <https://doi.org/10.3390/s16122010>
- Goodbred SL Jr, Hine AC (1995) Coastal storm deposition: saltmarsh response to a severe extratropical storm, March 1993, westcentral Florida. *Geology* 23:679–682

- Grimm EC (1992) Tilia software. Illinois State Museum, Springfield
- Hassan GS, De Francesco CG, Díaz MC (2020) Actualistic taphonomy of freshwater diatoms: Implications for the interpretation of the Holocene record in Pampean shallow lakes. In: Martínez S, Rojas A, Cabrera F (eds) Actualistic taphonomy in South America. Topics in Geobiology. Springer, Cham. https://doi.org/10.1007/978-3-030-20625-3_6
- Hine AC, Belknap DF, Hutton JG, Osking EB, Evans MW (1988) Recent geological history and modern sedimentary processes along an incipient, low-energy, epicontinental-sea coastline: Northwest Florida. *J Sediment Petrol* 58:567–579
- Jovanovska E, Phillips N, Tyree M (2019) *Diploneis calcilacustris*. In: Diatoms of North America. Retrieved October 13, 2020, from <https://diatoms.org/species/diploneis-calcilacustris>
- Juggins S (2017) Rioja: Analysis of Quaternary science data, R Package Version, 0.9–21
- Kemp AC, Vane CH, Horton BP, Culver SJ (2010) Stable carbon isotopes as potential sea-level indicators in salt marshes, North Carolina, USA. *Holocene* 20:623–636
- Kirwan ML, Megonigal JP (2013) Tidal wetland stability in the face of human impacts and sea-level rise. *Nature* 504:53–60
- Kirwan ML, Guntenspergen GR, d'Alpaos A, Morris JT, Mudd SM, Temmerman S (2010) Limits on the adaptability of coastal marshes to rising sea level. *Geophys Res Lett* 37:L23401. <https://doi.org/10.1029/2010GL045489>
- Kirwan ML, Temmerman S, Skeehan EE, Guntenspergen GR, Fagherazzi S (2016) Overestimation of marsh vulnerability to sea level rise. *Nat Clim Change* 6:253–260
- Klotzbach PJ, Schreck CJ III, Compo GP, Bowen SG, Oliver ECJ, Bell MM (2021) The record-breaking 1933 Atlantic Hurricane season. *B Am Meteorol Soc* 102:E446–E463. <https://doi.org/10.1175/BAMS-D-19-0330.1>
- Kokociński M, Szczucinski W, Zgrundo A, Ibragimow A (2009) Diatom assemblages in 26 December 2004 Tsunami deposits from coastal zone of Thailand as sediment provenance indicators. *Pol J Environ Stud* 18:93–101
- Krishnaswamy S, Lal D (1978) Radionuclide limnology. In: Lerman A (ed) *Lakes: Chemistry, Geology, Physics*. Springer-Verlag, New York, pp 153–177
- Krishnaswamy S, Lal D, Martin JM, Meybeck M (1971) Geochronology of lake sediments. *Earth Planet Sc Lett* 11:407–414
- Lamb AL, Wilson GP, Leng MJ (2006) A review of coastal palaeoclimate and relative sea-level reconstructions using $\delta^{13}\text{C}$ and C/N ratios in organic material. *Earth Sci Rev* 75:29–57
- Langston AK, Kaplan DA, Putz FE (2017) A casualty of climate change? Loss of freshwater forest islands on Florida's Gulf Coast. *Glob Change Biol* 23:5383–5397. <https://doi.org/10.1111/gcb.13805>
- Legendre P, Gallagher ED (2001) Ecologically meaningful transformations for ordination of species data. *Oecologia* 129:271–280. <https://doi.org/10.1007/s004420100716>
- Leonard LA, Hine AC, Luther ME, Stumpf RP, Wright EE (1995) Sediment transport processes in a west-central Florida open marine marsh tidal creek: the role of tides and extra tropical storms. *Estuar Coast Shelf S* 41:225–248
- Lowe R, Manoylov K (2011) *Cyclotella distinguenda*. In: Diatoms of North America. Retrieved Oct 13, 2020, from https://diatoms.org/species/cyclotella_distinguenda
- Mandal M, Żelazna-Wieczorek J, Sen Sarkar N (2020) New diatom taxa for the Indian Sundarbans found in short sediment cores. *Diatom Res* 35:17–35. <https://doi.org/10.1080/0269249X.2020.1716851>
- Mattson RA, Frazer TK, Hale JA, Blitch SB, Ahijevych L (2007) The Florida big bend. In: Handley L, Altsman D, DeMay R (eds) *Seagrass status and trends in the Northern Gulf of Mexico: 1940–2002*. U.S. Geological Survey scientific investigations report 2006–5287 and U.S. Environmental Protection Agency 855-R-04–003. 267 p
- McQuoid MR, Nordberg K (2002) The Diatom *Paralia sulcata* as an environmental indicator species in coastal sediments. *Estuar Coast Shelf Sci* 56:339–354. <https://doi.org/10.1006/ecss.2002.0974>
- Meirland A, Gallet-Moron E, Rybarczyk H, Dubois F, Charberrie O (2015) Predicting the effects of sea level rise on salt marsh plant communities: does vegetation age matter more than sea level? *Plant Ecol Evol* 148:5–18
- Meyers PA, Teranes JL (2001) Sediment organic matter. In: Last WM, Smol JP (eds) *Tracking environmental changes using lake sediment, physical and geochemical methods*, vol 2. Kluwer Academic, Dordrecht, pp 239–270
- Mitchum G, Dutton A, Chambers DP, Wdowski S (2017) Sea level rise. In: Chassignet EP, Jones JW, Misra V, Obeysekera J (eds) *Florida's climate: changes, variations, & impacts*. Florida Climate Institute, Gainesville, FL, pp 557–578. <https://doi.org/10.17125/fci2017.ch19>
- Möller I, Spencer T, French JR, Leggett DJ, Dixon M (1999) Wave transformation over salt marshes: a field and numerical modelling study from North Norfolk, England. *Estuar Coast Shelf Sci* 49:411–426
- Moore WS (1984) Radium isotope measurements using germanium detectors. *Nucl Instrum Methods Phys Res* 223:407–411
- Morris JT, Sundareshwar PV, Nietch CT, Kjerfve B, Cahoon DR (2002) Responses of coastal wetlands to rising sea level. *Ecology* 83:2869–2877
- Mudd SM, D'Alpaos A, Morris JT (2010) How does vegetation affect sedimentation on tidal marshes? Investigating particle capture and hydrodynamic controls on biologically mediated sedimentation. *J Geophys Res* 115:F03029. <https://doi.org/10.1029/2009JF001566>
- NOAA Center for Operational Oceanographic Products and Services (2019) Relative sea level trend, station 8727520, Cedar Key, Florida. National Ocean Services website, https://tidesandcurrents.noaa.gov/sltrends/sltrends_station.shtml?id=8727520
- Nicholls RJ, Wong PP, Burkett VR, Codignotto JO, Hay JE (2007) Coastal systems and low-lying areas. In: Parry ML, Canziani OF, Palutikof JP, van der Linden PJ, Hanson CE (eds) *Climate Change 2007: Impacts adaptation and vulnerability*. Contribution of working group II to the fourth assessment report of the intergovernmental panel on climate change. Cambridge University Press, Cambridge, UK, pp 315–356

- Oksanen J, Blanchet FG, Friendly M, Kindt R, Legendre P, McGinn D, Minchin PR, O'Hara RB, Simpson GL, Solyomos P, Stevens MHH, Szoecs E, Wagner H (2019) Vegan: community ecology package. R Package Version 2:5–6
- Parsons ML (1998) Salt marsh sedimentary record of the landfall of hurricane andrew on the Louisiana coast: diatoms and other paleoindicators. *J Coastal Res* 14:939–950
- R Core Team (2020) R: A language and environment for statistical computing
- Raabe EA, Stumpf RP (2016) Expansion of tidal marsh in response to sea-level rise: Gulf Coast of Florida, USA. *Estuaries Coasts* 39:145–157
- Riaux-Gobin C, Witkowski A, Igersheim A, Lobban CS, Al-Handal AY, Compère P (2018) *Planolithidium juandenoense* sp. nov. (Bacillariophyta) from Juan de Nova (Scattered Islands, Mozambique Channel) and other tropical environments: a new addition to the *Planolithidium delicatulum* complex. *Fottea* 18:106–119
- Round FE (1981) The ecology of the algae. Cambridge University Press, Cambridge, England
- Saintilan N, Wilson NC, Rogers K, Rajkaran A, Krauss KW (2014) Mangrove expansion and salt marsh decline at mangrove poleward limits. *Glob Change Biol* 20:147–157
- Sanger D, Parker C (2016) Guide to the salt marshes and tidal creeks of the Southeastern United States. South Carolina department of natural resources. <https://www.saltmarshguide.org/>
- Schelske CL, Peplow A, Brenner M, Spencer CN (1994) Low-background gamma counting: applications for ^{210}Pb dating of sediments. *J Paleolimnol* 10:115–128
- Seavey JR, Pine WE III, Frederick P, Sturmer L, Berrigan M (2011) Decadal changes in oyster reefs in the big bend of Florida's Gulf coast. *Ecosphere* 2:1–14. <https://doi.org/10.1890/ES11-00205.1>
- Sims PA, Crawford RM (2017) Earliest records of *Ellerbeckia* and *Paralia* from *cretaceous* deposits: a description of three species, two of which are new. *Diatom Res* 32:1–9
- Smoak JM, Breithaupt JL, Smith TJ III, Sanders CJ (2013) Sediment accretion and organic carbon burial relative to sea-level rise and storm events in two mangrove forests in Everglades National Park. *Catena* 104:58–66
- Spaulding SA, Potapova MG, Bishop IW, Lee SS, Gasperak TS, Jovanoska E, Furey PC, Edlund MB (2022) Diatoms.org: supporting taxonomists, connecting communities. *Diatom Res* 36(4):291–304. <https://doi.org/10.1080/0269249X.2021.2006790>
- Stancheva R (2019) *Cocconeis cascadenensis*, a new monoraphid diatom from mountain streams in Northern California, USA. *Diatom Res* 33:471–483. <https://doi.org/10.1080/0269249X.2019.1571531>
- Taffs KH, Saunders KM, Logan B (2017) Diatoms as indicators of environmental change in estuaries. In: Weckström K, Saunders K, Gell P, Skilbeck C (eds) Applications of paleoenvironmental techniques in estuarine studies. Developments in paleoenvironmental research. Springer, Dordrecht, pp 277–294. https://doi.org/10.1007/978-94-024-0990-1_11
- Tanimura Y, Sato H (1997) *Pseudopodosira kosugii*: a new Holocene diatom found to be a useful indicator to identify former sea-levels. *Diatom Res* 12:357–368
- Tiner RW (2013) Tidal wetlands primer: an introduction to their ecology, natural history, status, and conservation. University of Massachusetts Press, ProQuest Ebook Central, <http://ebookcentral.proquest.com/lib/knowledgecenter/detail.action?docID=4533173>
- Vaughn DR, Bianchi TS, Shields MR, Kenney WF, Osborne TZ (2020) Increased organic carbon burial in northern Florida mangrove-salt marsh transition zones. *Global Biogeochem Cy* 34:e2019GB006334. <https://doi.org/10.1029/2019GB006334>
- Vaughn DR, Bianchi TS, Shields MR, Kenney WF, Osborne TZ (2021) Blue carbon soil stock development and estimates within Northern Florida wetlands. *Front Earth Sci*. <https://doi.org/10.3389/feart.2021.552721>
- Vos PC, de Wolf H (1993) Diatoms as a tool for reconstructing sedimentary environments in coastal wetlands; methodological aspects. *Hydrobiologia* 269:285–296
- Wang L, Bianchette TA, Liu KB (2019) Diatom evidence of a paleohurricane-induced coastal flooding event in Weeks Bay, Alabama, USA. *J Coastal Res* 35:499–508
- Wetzel CE, Sar EA, Sunesen I, Van de Vijver B, Ector L (2017) New combination and typification of Neotropical *Cosmioneis* species (Cosmioneidaceae). *Diatom Res* 32:229–240. <https://doi.org/10.1080/0269249X.2017.1316776>
- Williams K, Ewel KC, Stumpf RP, Putz FE, Workman TW (1999) Sea level rise and coastal forest retreat on the west coast of Florida, USA. *Ecology* 80:20452063
- Wilson AM, Evans T, Moore W, Schutte CA, Joye SB, Hughes AH, Anderson JL (2015) Groundwater controls ecological zonation of salt marsh macrophytes. *Ecology* 96:840–849. <https://doi.org/10.1890/13-2183.1>
- Witkowski A, Lange-Bertalot H, Metzeltin D (2000) Diatom flora of marine coasts I. *Iconographia Diatomologica*. ARG Gantner Verlag 7:1–925
- Wright EE, Hine AC, Goodbred SL Jr, Locker SD (2005) The effect of sea-level and climate change on the development of a mixed siliciclastic-carbonate, deltaic coastline: Suwannee River, Florida, USA. *J Sediment Res* 75:621–635
- Yu Q, Wang F, Li X, Yan W, Li Y, Lv S (2018) Tracking nitrate sources in the Chaohu Lake, China, using the nitrogen and oxygen isotopic approach. *Environ Sci Pollut Res Int* 25:19518–19529. <https://doi.org/10.1007/s11356-018-2178-9>
- Zedler JB, Kercher S (2005) Wetland resources: status, trends, ecosystem services, and restorability. *Annu Rev Environ Resour* 30:39–74

Publisher's Note Springer Nature remains neutral with regard to jurisdictional claims in published maps and institutional affiliations.

Springer Nature or its licensor (e.g. a society or other partner) holds exclusive rights to this article under a publishing agreement with the author(s) or other rightsholder(s); author self-archiving of the accepted manuscript version of this article is solely governed by the terms of such publishing agreement and applicable law.